Research Article

Received: 11 December 2015 Revised: 7 March 2016 Accepted article published: 7 April 2016 Published online in Wiley Online Library: 5 May 2016

(wileyonlinelibrary.com) DOI 10.1002/jctb.4992

Comparative activity of CdS nanofibers superficially modified by Au, Cu, and Ni nanoparticles as co-catalysts for photocatalytic hydrogen production under visible light

Socorro Oros-Ruiz,[a*] Agileo Hernández-Gordillo,[b] Cinthia García-Mendoza,[a] Arturo A Rodríguez-Rodríguez[c] and Ricardo Gómez[a]

Abstract

BACKGROUND: The use of CdS as a catalyst under visible light for hydrogen production has attracted much attention owing to its ability to perform the photocatalytic hydrogen production under visible light; the use of noble metals as co-catalysts has been reported as an effective method to increase their efficiency. This work compares the activity of CdS catalysts using different metals as co-catalysts supported on its surface, such as gold, and non-noble metals such as Cu and Ni, enhancing the photocatalytic response.

RESULTS: The photodeposition method was used to support Au, Cu and Ni nanoparticles on the CdS to perform the photocatalytic evolution of hydrogen in the presence of visible light. The photodeposition method for these metals produced a mixture of oxidation states for the different metals evaluated (Au, Cu and Ni), being partially oxidized and partially in metallic form. Different metal loadings were analyzed to perform this reaction, the most active material obtained was Ni/CdS (10083 μmol h^{-1} g^{-1}) at metal loadings of 1.0% wt.% improving the photoactivity of bare support CdS by a factor of 15. Au and Cu improved the photoactivity of CdS semiconductor by factors of 6 and 2, respectively.

CONCLUSIONS: The presence of metal co-catalysts on CdS nanofibers increased the photocatalytic activity for hydrogen production under visible light. These results show that Ni can be an efficient co-catalyst enhancing the photoactivity of CdS semiconductors at low metal loadings that may overcome the use of noble metals as co-catalysts.

Keywords: CdS semiconductors; hydrogen production; photocatalysis; visible light

INTRODUCTION

The use of CdS semiconductors for photocatalytic applications has attracted much attention since it can be activated in the visible light region; specifically, it has recently been reported for photocatalytic hydrogen production.[1–3] Different routes of synthesis[4–8] leading to particular structures and morphologies,[9] such as nanospheres[10] nanorods,[11] nanofibers,[12] nanowires,[13] nanoflowers[14,15] have been obtained and reported since this semiconductor has the advantage of absorbing throughout the visible region from 300 to 500 nm. Different modifications have been proposed for this photocatalysts to improve its performance. As has been reported, the formation of a heterojunction using TiO_2,[16] the deposition of noble metals such as Pt on its surface,[17,18] non-noble metals such as copper[19] and nickel;[20] and recently the formation of Au@CdS core shell nanoparticles on TiO_2 have been evaluated for hydrogen production under visible light.[21] Among the efforts to improve the photocatalytic activity of semiconductors, several strategies to increase the response under visible light and to avoid the recombination of the h^+ e^- pair, have been used. These include forming composites with graphenes;[3] mixing with metal oxides to prevent e^- h^+ recombination by attracting the electrons to the surface of the semiconductor, acting as electron traps; and also the use of nanosized semiconductor nanoparticles to perform photocatalytic water splitting in the presence of visible light.[22] In the present work, photocatalytic hydrogen production under visible light using metal nanoparticles of Au, Cu, and Ni photodeposited on CdS, is investigated and compared in order to evaluate the effect of each metal as co-catalysts and the optimal

* *Correspondence to: S Oros-Ruiz, Universidad Autónoma Metropolitana-Iztapalapa, Departamento de Química, ECOCATAL, Av. San Rafael Atlixco No. 186, C.P. 09340, México, DF, México. Email: coco.oros@yahoo.com*

a *Universidad Autónoma Metropolitana-Iztapalapa, Departamento de Química, ECOCATAL, Av. San Rafael Atlixco No. 186, C.P. 09340, México, DF, México*

b *Instituto de Investigaciones en Materiales, Universidad Nacional Autónoma de México, Circuito exterior S/N, Ciudad Universitaria, CP 04510 México, D.F., Coyoacán, México*

c *Centro de Investigación en Materiales Avanzados, S. C. (CIMAV), Unidad Monterrey, Alianza Norte 202, Parque de Investigación e Innovación Tecnológica, 66600 Apodaca, Nuevo León, México*

metal loading. The photocatalysts were characterized by UV-Vis diffuse reflectance, XRD, N_2 physisorption, TEM and XPS. The photocatalytic activity of the materials was evaluated using an ethanol/water solution 50–50% vol., the irradiation source was a set of four blue-LED lamps with primary emission at 450 nm.

EXPERIMENTAL SECTION

Synthesis of CdS nanofibers

The CdS nanofibers were prepared by the precipitation method[12] using a mixture of solvents containing 10 vol.% of H_2O, 60 vol.% of ethylenediamine (Aldrich) and 30 vol.% of *n*-butanol (Baker). In a typical procedure, appropriate amounts of $Cd(NO_3)_2H_2O$ (Reasol) were dissolved in the aqueous solution of *n*-butanol at room temperature at constant stirring for 15 min; then ethylenediamine was added dropwise. Afterwards carbon disulfide (CS_2, Aldrich) was added dropwise, maintaining a stoichiometry molar ratio S:Cd of 1:1. The transparent solution obtained was heated at boiling point (90–110 °C) for 1 h and subsequently cooled at room temperature under vigorous magnetic stirring. Finally, the resulting yellow precipitate was collected by filtration, washed several times with an ethanol–water solution and dried at 80 °C for 1 h. The final solids were recovered and stored.

Photodeposition of metal nanoparticles on CdS nanofibers

Deposition of the different metal nanoparticles on the CdS surface was performed by the photodeposition method[23] using four blue-LED lamps of a primary emission at 450 nm. Briefly, 500 mg of the CdS nanofibers were put in distilled water and methanol (Caledon 99.8%) at a concentration 1 mol L^{-1} in a final volume of 500 mL. In this procedure, the quartz reactor was placed in dark conditions, and deoxygenated for 30 min under N_2 flow (100 mL min^{-1}) and constant stirring, then the metallic precursor was added to the suspension; $HAuCl_4 \cdot 3H_2O$ (Aldrich 99.99%), $Cu(NO_3)_2 \cdot 2.5H_2O$ (Aldrich 99%) or $Ni(OCOCH_3)_2 \cdot 4H_2O$ (Aldrich 98.5%). Afterwards the four blue-LED lamps were turned on and the samples left for 2 h under irradiation. Finally, the suspensions were centrifuged and the materials collected and washed with distilled water. After drying at 80 °C for 12 h, the samples were stored at room temperature in a desiccator under vacuum, away from light in order to prevent any alteration. The different metal loadings photodeposited on the CdS surface were 0.5, 1.0 and 1.5 wt.%

Characterization

To estimate the band-gap energy of the photocatalysts (E_g), a Cary 100 Scan spectrophotometer by Varian equipped with an integrating sphere (Labsphere DRA-CA-30I) was used. The elemental analysis of the catalysts was determined by energy dispersive X-ray fluorescence spectroscopy using a JSX1000S JEOL Spectrometer. The analysis of metal particle size was performed by transmission electron microscopy (TEM) using a JEOL JEM 2010 operated at 200 keV. The structure of the CdS support was determined by X-ray powder diffraction using a D8 Advance Bruker X-ray diffractometer with Cu Kα radiation of 1.5406 Å (35 kV 25 mA). The scanning rate was 0.03° s^{-1} in the 2θ range from 5° to 80°. N_2 adsorption–desorption isotherms at −196 °C were obtained using a Quantachrome Autosorb-3B equipment. The specific surface areas were calculated by the BET method. Prior to N_2 admission to the cell all the semiconductors were degassed at 80 °C for 24 h under vacuum. The oxidation states of the different metal nanoparticles on the CdS nanofibers were analyzed by XPS on a Thermo Scientific Escalab 250 Xi instrument. The working pressure was ~10^{-10} mbar, and the photoelectrons were generated with an Al Kα (1486.68 eV) source. The X-ray voltage used was 14 kV and the power 350 W. The spectra were obtained using pass energy of 50 eV, and the recorded photoelectron peaks were curve fitted using the Thermo Avantage software V 5.41. The binding energies were referenced to the C (1 s) peak fixed at 284.8 eV.

Table 1. Parameters of the CdS photocatalysts containing different metals as co-catalysts (1 wt.%)

Photocatalyst	Metal loading (wt.%)	E_g (eV)	Surface area (m^2 g^{-1})	Particle size (nm)	Hydrogen production (μmol h^{-1} g^{-1}).
CdS	---	2.5	173.1	---	636
Au/CdS 1.0 wt.%	1.2	2.4	151.2	6.5	3602
Cu/CdS 1.0 wt.%	1.2	2.4	167.4	5.5	1186
Ni/CdS 1.0 wt.%	1.1	2.4	137.4	5.2	10083

Evaluation of the photocatalytic activity for hydrogen production

The photocatalytic activity of the CdS nanofibers and the CdS materials containing metal nanoparticles Au/CdS, Ni/CdS and Cu/CdS at different metal loadings of 0.5, 1.0 and 1.5 wt.%, were evaluated in a homemade photoreactor containing 20 mg of the catalyst in 200 mL of a water–ethanol mixture (1:1 vol. ratio). The irradiation source was a set of four blue-LED lamps of 3 W with emission at 450 nm. The determinations of hydrogen were made in a Shimadzu G-08 gas chromatograph with a thermal conductivity detector (TCD) using a Shincarbon packed column (2 m length, 1 mm ID and 25 mm OD). The reactions were monitored for 6 h. To assure adsorption/desorption equilibrium, the system was stirred in the dark for 30 min and degassed by bubbling nitrogen prior to the photochemical reaction.

RESULTS AND DISCUSSION

Elemental analysis

In Table 1 the measured metal loadings on the CdS nanofibers containing 1 wt.% are reported, and present good agreement with the nominal values calculated indicating that the metallic precursors were efficiently deposited by the photodeposition method.

Structural analysis of the CdS nanofibers

The main diffraction peaks of the CdS materials are presented in Fig. 1, exhibiting the planes (100), (002) (101) (102) (210) (103) (212) corresponding to the hexagonal phase of CdS (JCPD 41-1049) with the lattice parameters (a = 4.1 Å and c = 6.7 Å). The high relative intensity of the diffraction peak (002) plane indicates preferential growth along the c-axis of the hexagonal phase.[8] Diffractograms of the superficially modified materials by metal nanoparticles (Cu, Ni or Au) did not present any obvious change in the crystalline structure of the hexagonal CdS, and no evidence of metal nanoparticles is observed by this characterization technique since the metal loadings are below 1 wt.% (Table 1).

Particle size distribution

Figure 2 shows micrographs of the CdS materials and the CdS nanofibers containing metal nanoparticles. These images show

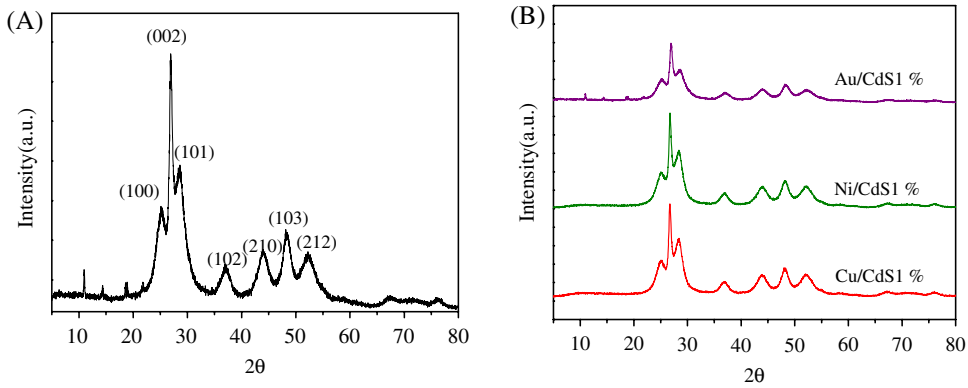

Figure 1. X-ray diffractograms of (A) bare CdS and (B) CdS containing different metal nanoparticles as co-catalysts (1 wt.%).

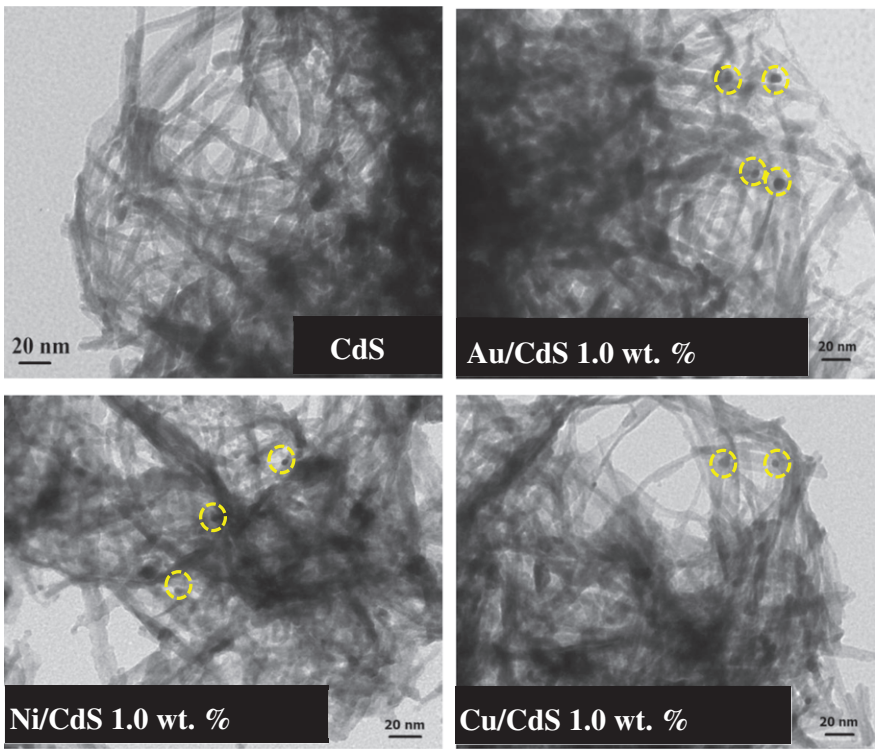

Figure 2. TEM images of the CdS photocatalysts and CdS containing different metals as co-catalysts (1 wt.%).

agglomerated fiber-like morphologies for the CdS with diameters between 6 and 12 nm, and lengths above 100 nm. In these images, the presence of small rounded particles with diameters between 4 and 9 nm can be observed, corresponding to the metal nanoparticles photodeposited on the CdS nanofibers surface; the average particle size of these metal nanoparticles is 5 nm (Table 1). These results indicate that photodeposition of the metal nanoparticles allowed good control and good dispersion of these metallic nanoparticles over the surface of the CdS nanofibers.

Determination of the oxidation state of the metal nanoparticles

Determination of the oxidation state of the different metal nanoparticles used as co-catalysts on the CdS nanofibers was studied by X-ray photoelectron spectroscopy; in order to reduce the noise in the XPS spectra, the samples selected were those containing 1.5 wt.%. Figure 3 shows the XPS spectra of samples previously dried at 80 °C under air flow. The position of the Au 4f peaks showed the characteristic signal 4f $^{7/2}$ in the range 82.8 and 83.2 eV, Fig. 3(A). The position of the signal is slightly lower than that of bulk gold, and it is usually assigned to small gold particles in the metallic state. The spectrum was deconvoluted into several components, the Au^0 $4f_{7/2}$ peaks were detected at a range of binding energy (BE) of 83.0–83.1 eV, typical of metallic gold; and the spectra binding energies at 86.2 and 89.9 eV were attributed to the presence of Au in the form of Au^{3+}.[24] The doublet corresponding to metallic gold (Au^0) is located at 84 eV (Au $4f_{7/2}$) and 87.5 eV (Au $4f_{5/2}$); the oxidized gold signal appears at higher binding energies (Au^I $4f_{7/2}$ at 84.7 eV and Au^{III} $4f_{7/2}$ at 85.2 eV).[25] From these spectra we can observe that the photoreduction of gold was not totally completed, resulting in higher amounts of oxidized gold than metallic gold (Fig. 3(A)).

The XPS spectra of the CdS material containing Cu nanoparticles is presented in Fig. 3(B), and for the region 960–920 eV, the peak

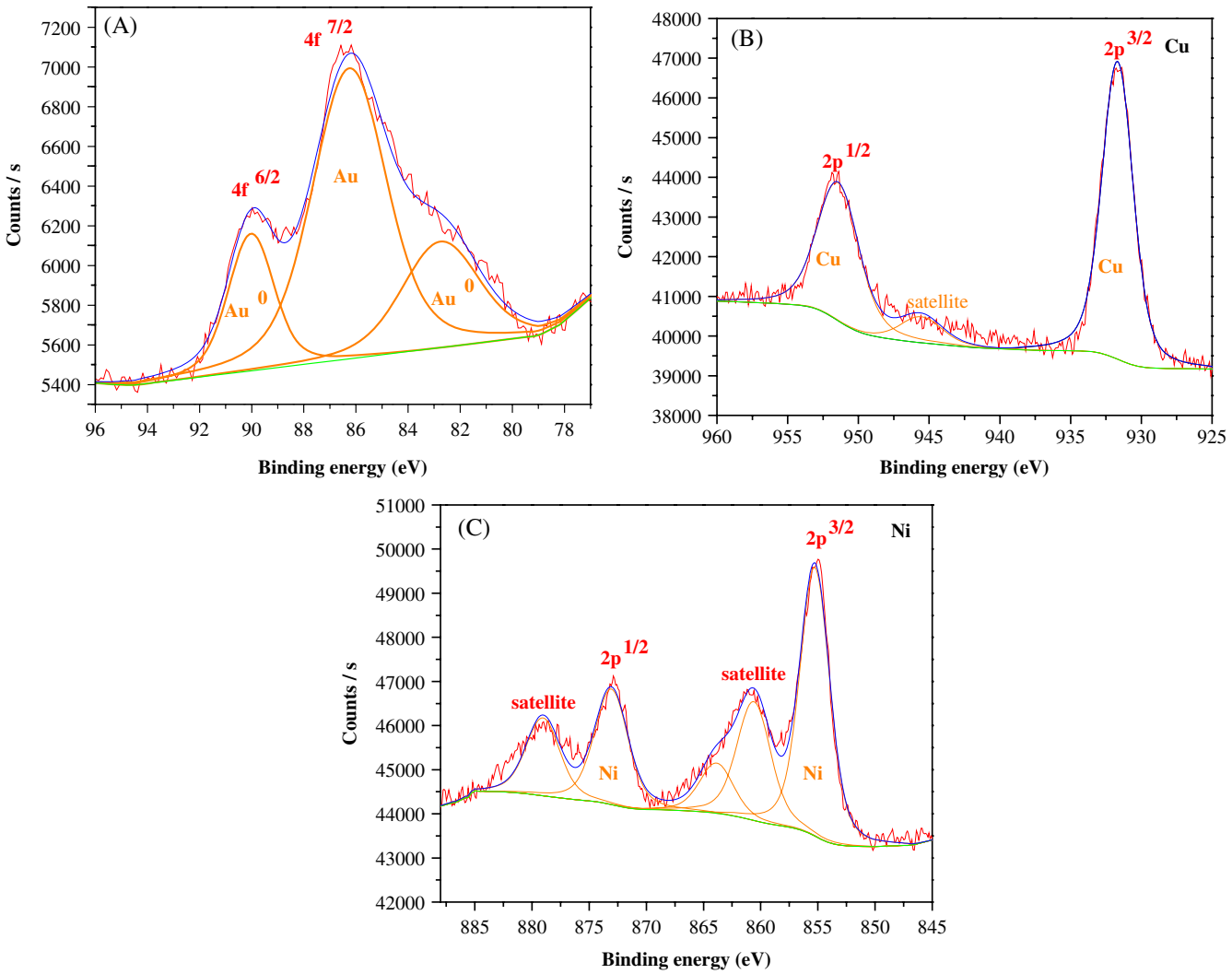

Figure 3. XPS of the different CdS nanofiber catalysts containing metal nanoparticles evaluated for hydrogen production: (A) Au/CdS, (B) Cu/CdS, and (C) Ni/CdS at metal loadings of 1.5 wt.%.

for the Cu 2p core level is observed. The deconvolution of the Cu 2p signal was resolved in Cu $2p_{1/2}$ and Cu $2p_{3/2}$ core level peaks, identifying the Cu^0 and Cu^{1+} species[26] (Fig. 3(B)).

The XPS spectra of the CdS materials containing Ni nanoparticles are presented in Fig. 3(C), where the signals in the 2d region correspond to Ni $2p_{3/2}$ and Ni $2p_{1/2}$ at 854.9 and 872.7 eV and the satellite peaks at 860.9 and 878.7 eV.[27] These signals correspond to NiO and/or $Ni(OH)_2$, Fig. 3(C).[28]

Textural properties of CdS nanofibers

The nitrogen adsorption–desorption isotherms of the CdS sample and the Au/CdS, Ni/CdS and Cu/CdS for the metal loadings of 1 wt.% are presented in Fig. 4. According to the IUPAC classification, the isotherms correspond to type II, characteristic of materials where the interactions between the adsorbate and the adsorbent are weak; however, the adsorbed volume slightly decreased when the metal nanoparticle was deposited. The specific surface area of the CdS was 173 $m^2\ g^{-1}$ and it decreased to 167, 151 and 137 $m^2\ g^{-1}$ for Cu/CdS, Au/CdS and Ni/CdS, respectively, at metal loadings of 1 wt.%. The CdS area obtained corresponds to the interstitial spaces between the fibers, and the small decrease in the surface area presented by the CdS nanofibers superficially modified by metal nanoparticles is probably attributable to stacking of the CdS support due to the different mechanical effects of the several washes, centrifugations and heating during the photoreduction process for deposition of the different metal nanoparticles.

Optical properties of photocatalysts

The selected UV-Vis diffuse reflectance spectra of CdS nanofibers and CdS materials containing metal nanoparticles (1 wt.%) were analyzed and are presented in Fig. 5. The bare CdS semiconductor presents absorption in the range 400–500 nm, attributed to the intrinsic bang-gap transition of electrons from the valence band to the conduction band of CdS. The material containing gold nanoparticles (Au/CdS) presents wide absorption in the visible region from 500 nm to the IR region at 800 nm. This signal is partly generated by the plasmonic resonance of light on the surface of the small amount of formed metallic nanoparticles at 550 nm, besides the wide absorption from 400 up to 800 nm, attributed to the gold oxide species Au(III)[29] attached to the CdS surface. For the sample Cu/CdS, wide absorption throughout the visible region due to the contribution in the visible region of the CuO_x species located in the visible range (400 to 800 nm).[30] The Ni/CdS materials presented lower absorption in the visible region. The bandgap

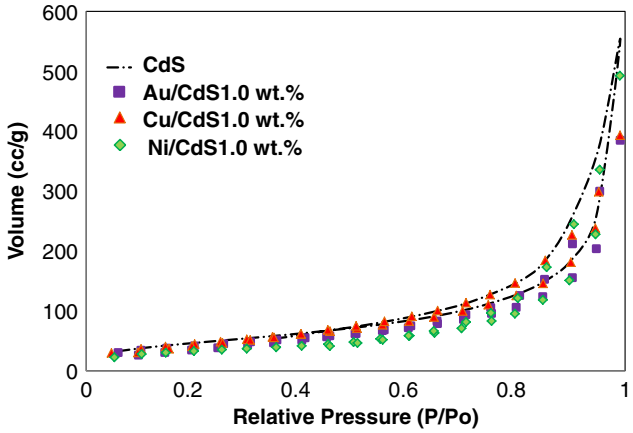

Figure 4. N_2 adsorption–desorption isotherm of the CdS and the CdS support modified by different metal nanoparticles (1 wt.%).

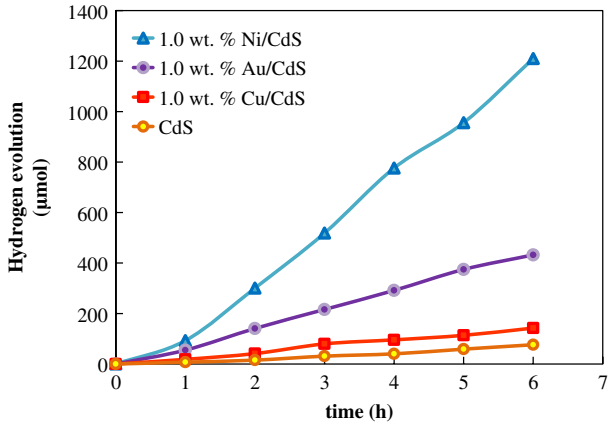

Figure 6. Hydrogen evolution of CdS nanofibers with different metal nanoparticles as co-catalysts (1 wt.%).

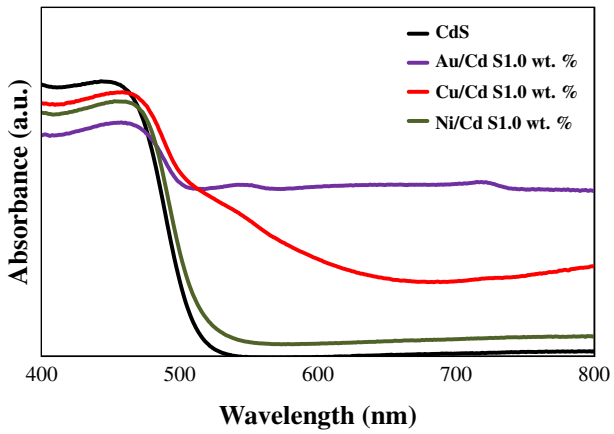

Figure 5. UV-Vis absorption spectra of CdS and CdS photocatalysts with different metals evaluated as co-catalysts at the optimal metal loading of 1 wt.%.

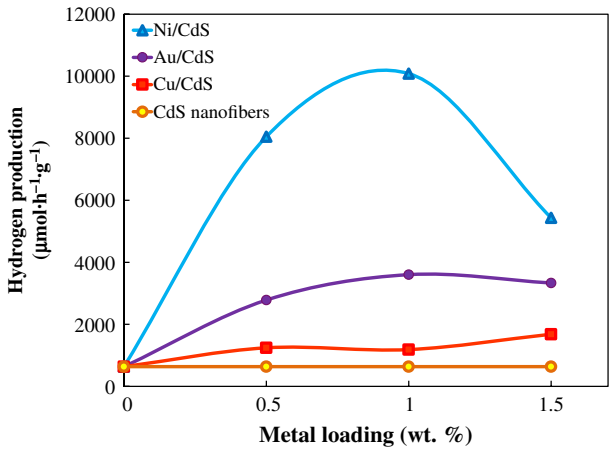

Figure 7. Photocatalytic hydrogen evolution for CdS photocatalyst using different metal nanoparticles as co-catalysts at 0.5, 1.0 and 1.5 wt.%.

energies of these materials were estimated by the Kubelka–Munk (KM) method using the theory of optical absorption for indirect allowed transitions (2.4–2.5 eV) and are reported in Table 1.

Hydrogen production of CdS nanofibers containing metal nanoparticles

Evaluation of the photocatalytic hydrogen production of CdS using different metals as co-catalysts (Au, Cu and Ni) was performed under visible light and results are shown in Fig. 6. As shown by XPS, the photodeposition method allowed the synthesis of metals in a mixture of metallic and oxidized states for the different metals. As has also been studied and reported in previous works,[25] a mixture of 75% of metallic gold and 25% oxidized gold of (Au^+/Au^{3+}) is formed using this deposition method for gold nanoparticles. Ni after the photodeposition method forms $Ni(OH)_2$, and during the photocatalytic reaction may lead to NiO.[31] Metals such as Ni and Cu nanoparticles are known to be easily oxidized in aqueous medium and therefore the presence of these metals corresponded to NiO and CuO and Cu_2O.[28] The combination of CdS with these NiO nanoparticles as co-catalysts modified the semiconductor surface of the conduction band (CB) levels to enhance the charge transfer on the surface at the junction of the photodeposited metals and the CdS surface; these transferred electrons are able reduce aqueous protons and to avoid the recombination of h^+ e^-, so that Ni co-catalyst presented the highest catalytic effect under visible light. Au in its metallic form has been reported to be a very efficient co-catalysts for hydrogen production,[28] however, this deposition method led to a mixture of oxidation states that may have hindered its activity as co-catalyst. The presence of Cu as metallic Cu^0 and Cu_2O also improved the photoactivity of bare CdS but with less effect than Ni and Au nanoparticles.

The hydrogen evolution of the CdS nanofibers at metal loadings of 0.5, 1.0 and 1.5 wt.% of Au, Cu and Ni was evaluated, and the photoactivity was improved for all CdS materials containing metal co-catalysts. Optimal metal loading was 1.0 wt.%, and Ni was the best co-catalyst at every metal content evaluated. The optimal photocatalyst 1.0 Ni/CdS gave photoactivity 10083 μmol h^{-1} g^{-1}; in decreasing order of activity it was followed by the material Au/CdS (3600 μmol h^{-1} g^{-1}) and Cu/CdS (1185 μmol h^{-1} g^{-1}). All these materials reported an enhancement in the photoactivity over the bare photocatalyst CdS (636 μmol h^{-1} g^{-1}) as can be observed in Fig. 7.

CONCLUSIONS

The presence of metal co-catalysts on the surface of CdS nanofibers increased the photocatalytic activity for hydrogen

production under visible light. The photodeposition method for these metals produced a mixture of oxidation states for the different metals evaluated (Au, Cu and Ni), being partially oxidized and partially in metallic form. The most active material obtained was Ni/CdS (10083 μmol h^{-1} g^{-1}) at metal loadings of 1.0 wt.%, improving the photoactivity of the bare support CdS by a factor of 15. Au and Cu improved the photoactivity of CdS semiconductor by factors of 6 and 2, respectively. These results show that Ni can be used as an efficient co-catalyst, enhancing the photoactivity of CdS semiconductors at low metal loadings and can replace the use of noble metals as co-catalysts.

ACKNOWLEDGEMENTS

The authors thank CONACyT for the financial support through the project 253752 Apoyo al Fortalecimiento y Desarrollo de la Infraestructura Científica y Tecnológica 2015, and the SEP Proyect 103.5/15/14156. We are also grateful to Luis Gerardo Silva (CIMAV, S.C.) for the XPS measurements and assistance.

REFERENCES

1 He K, Wang M and Guo L, Novel CdS nanorod with stacking fault structures: preparation and properties of visible-light-driven photocatalytic hydrogen production from water. *Chem Eng J* **279**:747–756 (2015).
2 Majeed I, Nadeem A, Al-Oufi M, Nadeem MA, Waterhouse GIN, Badshah A *et al.*, On the role of the metal particle size and surface coverage for photo-catalytic hydrogen production: a case study of the Au/CdS system. *Appl Catal B: Environ* **182**:266–276 (2016).
3 Xu J, Wang L and Cao X, Polymer supported graphene-CdS composite with enhanced photocatalytic hydrogen production from water splitting under visible light. *Chem Eng J* **283**:816–25 (2016).
4 Ren B, Cao M, Zhang Q, Huang J, Zhao Z, Jin X *et al.*, Controllable synthesis of CdS nanowire by a facile solvothermal method and its temperature dependent photoluminiscent property. *J Alloy Compd* **659**:74–81 (2016).
5 Samadi-Maybodi A and Sadeghi-Maleki MR, *In situ* synthesis of high stable CdS quantum dots and their applications for photocatalytic degradation of dyes. *Spectrochim Acta A* **152**:156–164 (2016).
6 Fang S, Sun M, Zhou Y, Liang Q, Li Z and Xu S, Solvothermal synthesis of CdS QDs/MWCNTs nanocomposites with high efficient photocatalytic activity under visible light irradiation. *J Alloy Compd* **656**:771–776 (2016).
7 Kaviyarasu K, Manikandan E and Maaza M, Synthesis of CdS flower-like hierarchical microspheres as electrode material for electrochemical performance. *J Alloy Compd* **648**:559–263 (2015).
8 Hernández-Gordillo A, Tzompantzi F, Oros-Ruiz S, Torres-Martínez LM and Gómez R, Enhanced blue-light photocatalytic H_2 production usind CdS nanofiber. *Catal Comm* **45**:139–143 (2014).
9 Zhang B, Yao W, Huang C, Xu Q and Wu Q, Shape effects of CdS photocatalysts on hydrogen production. *Int J Hydrogen Energy* **38**:7224–7231 (2013).
10 Yao X, Liu T, Liu X and Lu L, Loading of CdS nanoparticles on the (101) surface of elongated TiO_2 nanocrystals for efficient visible-light photocatalytic hydrogen evolution from water splitting. *Chem Eng J* **255**:28–39 (2014).
11 Cao S, Wang CJ, Lv XJ, Chen Y and Fu WF, A highly efficient photocatalytic H_2 evolution system using colloidal CdS nanorods and nickel nanoparticles in water under visible light irradiation. *Appl Catal B Environ* **162**:381–391 (2015).
12 Hernández-Gordillo A, Oros-Ruiz S and Gómez R, Preparation of efficient cadmium sulfide nanofibers for hydrogen production using ethylenediamine ($NH_2CH_2CH_2NH_2$) as template. *J Colloid Inerf Sci* **451**:40–45 (2015).
13 Jang JS, Kim HG, Joshi UA, Jang JW and Lee JS, Fabrication of CdS nanowires decorated with TiO_2 nanoparticles for photocatalytic hydrogen production under visible light irradiation. *Int J Hydrogen Energy* **33**:5975–5980 (2008).
14 Tai G and Guo W, Sonochemistry-assisted microwave synthesis and optical study of single-crystalline CdS nanoflowers. *Ultrasound Sonochem* **15**:350–356 (2008).
15 Kong Q, Wu R, Feng X, Ye C, Hu G, Hu J *et al.*, Synthesis; characterization and growth mechanism of Au/CdS heterostructured nanoflowers constructed with nananorods. *J Alloy Compd* **509**:3048–3051 (2011).
16 Bai J, Li J, Liu Y, Zhou B and Cai W, A new glass substrate photoelectrocatalytic electrode for efficient visible-light hydrogen production: CdS sensitized TiO_2 nanotube arrays. *Appl Catal B: Environ* **95**:408–413 (2010).
17 Zhou X, Chen H, Sun Y, Zhang K, Fan X, Zhu Y *et al.*, Highly efficient light-induced hydrogen evolution from a stable Pt/CdS NPs-co-loaded hierchically porous zeolite beta. *Appl Catal B Environ* **152–153**:271–279 (2014).
18 Yao W, Song X, Huang C, Xu Q and Wu Q, Enhancing solar hydrogen production via modified photochemical treatment of Pt/CdS photocatalyst. *Catal Today* **199**:42–47 (2013).
19 Cheng WY, Yu TH, Chao KJ and Lu SY, Cu_2O-decorated CdS nanostructures for high efficiency visible light driven hydrogen production. *Int J Hydrogen Energy* **38**:9665–9672 (2013).
20 Wang H, Chen W, Zhang J, Huang C and Mao L, Nickel nanoparticles modified CdS-A potential photocatalyst for hydrogen production through water splitting under visible light irradiation. *Int J Hydrogen Energy* **40**:340–345 (2015).
21 Kim M, Kim YK, Lim SK, Kim S and In SI, Efficient visible light-induced H_2 production by Au@CdS/TiO_2 nanofibers: synergistic effect of core-shell structured Au@CdS and densely packed TiO_2 nanoparticles. *Appl Catal B Environ* **166–167**:423–431 (2015).
22 Cao S, Wang CJ, Lv XJ, Chen Y and Fu WF, A highly efficient photocatalytic H_2 evolution system using colloidal CdS nanorods and nickel nanoparticles in water under visible light irradiation. *App Catal B* **162**:381–391 (2015).
23 Oros-Ruiz S, Pedraza-Avella JA, Guzmán C, Quintana M, Moctezuma E, del Angel G, Gómez R and Pérez E, Effect of gold particle size and deposition method on the photodegradation of 4-chlorophenol by Au/TiO_2. *Top Catal* **54**:519–526 (2011).
24 Zhao J, Xu J, Zhang T, Di X, Ni J and Li X, Enhancement of Au/AC adetylene hydrochlorination catalyst activity and stability via nitrogen-modified activated carbon support. *Chem Eng J* **262**:1152–1160 (2015).
25 Hidalgo MC, Murcia JJ, Navío JA and Colón G, Photodeposition of gol don titanium dioxide for photocatalytic phenol oxidation. *Appl Catal B Environ* **397**:112–120 (2011).
26 López R, Gómez R and Llanos ME, Photophysical and photocatalytic properties of nanosized copper-doped titania sol-gel catalysts. *Catal Today* **148**:103–108 (2009).
27 Wagner CD, Riggs WM, Davis LE, Moulder JF and Mullenberg GE, *Handbook of X-ray Photoelectron Spectroscopy*, ed by Muilenberg GE. Perkin-Elmer Corp. (1979).
28 Oros-Ruiz S, Zanella R, Collins SE, Hernández-Gordillo A and Gómez R, Photocatalytic hydrogen production by Au-MxOy (M = Ag, Cu, Ni) catalysts supported on TiO_2. *Catal Comm* **47**:1–6 (2014).
29 Moreau F, Bond G and Taylor A, Gold on titania catalysts for the oxidation of carbon monoxide: control of pH during preparation with various gold contents. *J Catal* **231**:105-114 (2005).
30 Valero JM, Obregón S and Colón G, Active site considerations on the photoctalytic H_2 evolution performance of Cu-doped TiO_2 obtained by different doping methods. *ACS Catal* **4**:3320–3329 (2014).
31 Chen X, Chen W, Gao H, Yang Y and Shangguan W, *In situ* photodeposition of NiO_x on CdS for hydrogen production under visible light: Enhanced activity by controlling solution environment. *Appl Catal B* **152–153**:68–72 (2014).

